Springer Ser Chem Sens Biosens (2006) 4: 69–91
DOI 10.1007/5346_015

Published online: 25 May 2006

Molecular Interactions in SPR Sensors

Josef Štěpánek[1] (✉) · Hana Vaisocherová[2] · Marek Piliarik[2]

[1]Faculty of Mathematics and Physics, Charles University, Prague, Czech Republic
stepjos@karlov.mff.cuni.cz

[2]Institute of Radio Engineering and Electronics, Prague, Czech Republic

Keywords Association · Diffusion · Dissociation · Equilibrium constant · Flow cell · Mass transport · Rate constants · Reaction kinetics · Sensor · Surface plasmon resonance

Abbreviations

A Analyte (free reagent in solution)
B Complex of analyte and receptor
D Diffusion coefficient (coefficient of translational diffusion)
Da Damköhler number
h Flow cell height
k_a Association rate constant
k_d Dissociation rate constant
K Equilibrium association constant (binding affinity)
l Flow cell length
N_A Avogadro's number
PDE Fundamental equation of analyte transport inside flow cell (partial differential equation)
Pe Peclét number
R Receptor (binding target for the analyte immobilized at the sensor surface)
RU Units of the SPR sensor response (resonance units)
Re Reynolds number
w Flow cell width
[X] Molar concentration of X
x Space coordinate in direction of the analyte flow

y Space coordinate in direction perpendicular to the sensor surface
α Free analyte concentration ($\equiv [A]$)
α_0 Injected analyte concentration
β Surface concentration of receptor (moles per square area)
γ Surface concentration of complex (indexed for various types of complexes when necessary)
ξ Sensor response (in RU)
ξ_S Standard sensor response (in RU) corresponding to all receptor sites bound to analyte in 1 : 1 ratio

1 Introduction

Binding and/or unbinding of biomolecules at the active surface of an SPR biosensor is controlled by various mechanisms that result in variety of temporal profiles of the SPR biosensor response and in dependence on microenvironmental conditions. The determination of binding kinetics provides important new information about interacting molecules. This is commonly considered one of the greatest advantages of the SPR biosensor technique. Although in ideal cases an appropriate kinetic model of molecular interaction is able to completely describe the SPR biosensor response, in reality the influence of hydrodynamic conditions often has to be taken into account [1]. This chapter is devoted to molecular interaction models that correspond to the processes most frequently encountered at SPR biosensor surfaces. It also deals with hydrodynamic effects and their exact or approximate mathematical description.

2 Interaction Models

To quantitatively analyze the sensor response to interactions between the studied biomolecule (analyte) and the surface bound receptors, it is necessary to employ a relevant mathematical model. The core part of the model is a kinetic equation that describes how the temporal amounts of formed/dissociated complexes depend on the momentary local concentrations of the free analyte and the free binding sites of the receptors.

SPR biosensor experiments measure only relative changes in the molecular mass attached to the sensor surface from the beginning of the interaction being studied. The response ξ is then directly proportional to the concentration of the bound analyte (conditions that guarantee a linear sensor response are assumed throughout the chapter). In the case of a single type of analyte binding to the receptors in a 1 : 1 stoichiometric ratio, the response is proportional

to the concentration of the formed complexes:

$$\xi = \text{const}\, M_A \gamma\,, \tag{1}$$

where M_A is the mass of the analyte molecule and γ is the surface concentration of the formed complexes. It can be shown that for sufficiently high analyte concentrations, the sensor response will eventually reach its maximum value, which corresponds to all of the receptors being occupied. This response does not change measurably with further increases in the analyte concentration. Considering that the maximum possible response for the 1 : 1 stoichiometry is given by:

$$\xi_S = \text{const}\, M_A \beta\,, \tag{2}$$

where β is the surface concentration of receptors, it is widely useful to characterize the sensor response by its normalized value:

$$\xi/\xi_S = \gamma/\beta\,. \tag{3}$$

2.1 Pseudo First-Order Kinetics

Whenever we deal with analyte binding to receptors fixed at a sensor surface, the second order reaction model represents the basis of its description. This model concerns the situation when two partners, A and R, form a single complex AR. This can be, for instance, binding of an antigen to an antibody, docking of a substrate to an enzyme with a single binding pocket, or duplex formation by two complementary chains of nucleic acid. In the case of interactions at the sensor surface, we have to distinguish between the immobilized receptor R and the analyte A present in the solution. Two processes are considered by the model: (1) the association process whereby A and R bind to each other and create the immobilized complex AR and (2) the dissociation process whereby the complex AR dissociate into two parts, A and R. These processes are symbolized by:

$$\mathrm{A} + \mathrm{R} \rightarrow \mathrm{AR} \quad \text{and} \quad \mathrm{AR} \rightarrow \mathrm{A} + \mathrm{R}\,. \tag{4}$$

For the association, it is essential that A and R are in close proximity, i.e., their distance must be shorter than a critical radius. If this condition is satisfied, there is a certain probability that within a unit time interval A and R will form a complex. For a set of given environmental conditions (temperature, pressure, solvent properties) this probability is the same for all neighboring pairs of A and R, provided we do not consider microscopic conditions such as their mutual orientation or their instantaneous speeds of translation and rotation. For a given receptor the probability that any molecule of analyte appears within the critical distance is proportional to the concentration of A. The total number of associations per time interval in a particular region is proportional

to the total number of receptors involved, because they all can create a complex with the same probability. As a result, we obtain a relationship between the amount of the complexes γ formed per unit time, the instantaneous concentration of the free analyte $[A] = \alpha$, and the concentration of free receptors β–γ:

$$\frac{\mathrm{d}\gamma_\mathrm{a}}{\mathrm{d}t} = k_\mathrm{a}\alpha\left(\beta - \gamma\right) , \tag{5}$$

where k_a is a constant that characterizes the chemical reaction in the sense that it is independent of time and of the reactants concentrations. It is called the association or forward rate constant.

On the other hand, for each complex there is certain probability that within a unit time interval it will dissociate into A and R separated by a distance larger than the critical radius. This probability is the same for all complexes at the given conditions. The dissociation leads to a decrease of the complex concentration proportional to its instantaneous value:

$$\frac{\mathrm{d}\gamma_\mathrm{d}}{\mathrm{d}t} = - k_\mathrm{d}\gamma , \tag{6}$$

where k_d is called the dissociation or reverse rate constant. In a real system, both the association and dissociation processes occur simultaneously. It can be symbolically expressed as:

$$\mathrm{A} + \mathrm{R} \underset{k_\mathrm{d}}{\overset{k_\mathrm{a}}{\rightleftharpoons}} \mathrm{AR} . \tag{7}$$

The time dependence of the total complex concentration is then described by the summed effects of both processes:

$$\frac{\mathrm{d}\gamma}{\mathrm{d}t} = \frac{\mathrm{d}\gamma_\mathrm{a}}{\mathrm{d}t} + \frac{\mathrm{d}\gamma_\mathrm{d}}{\mathrm{d}t} = k_\mathrm{a}\alpha\left(\beta - \gamma\right) - k_\mathrm{d}\gamma . \tag{8}$$

Both quantities β and γ must be expressed in the same kind of local density. In the case of a solution phase reaction, we would understand them as molar concentrations, i.e., number of moles per unit volume. For receptors fixed on the sensor surface it is more straightforward to define them as surface concentrations, i.e., number of moles per unit area.

The solution of Eq. 8 depends strongly on how the concentration of the free analyte α is controlled. In the case of an active sensor surface surrounded by a solvent occupying certain closed volume V, the analyte can be injected as a highly concentrated solution [1, 2]. In the ideal case of a perfectly mixed solution, the effect of the injection can be described as an immediate jump in the analyte concentration from zero to a certain starting value α_0. During the consequent process the free analyte will be consumed by association with the receptor, while the sum of the free and bound analyte will be kept constant:

$$\alpha V + \gamma S = \alpha_0 V = \mathrm{const} , \tag{9}$$

where S is the sensor area. The temporary change in the complex concentration is then proportional to a quadratic polynomial of its instantaneous value (Fig. 1):

$$\frac{\mathrm{d}\gamma}{\mathrm{d}t} = k_\mathrm{a}\left(\alpha_0 - \frac{S}{V}\gamma\right)\left(\beta - \gamma\right) - k_\mathrm{d}\gamma\,. \tag{10}$$

At longer times, the solution of Eq. 10 converges to an equilibrium state $\left(\frac{\mathrm{d}\gamma}{\mathrm{d}t} = 0\right)$, which is characterized by the well-known equation:

$$K = \frac{k_\mathrm{a}}{k_\mathrm{d}} = \frac{\gamma_\mathrm{eq}}{\left(\alpha_0 - \gamma_\mathrm{eq}S/V\right)\left(\beta - \gamma_\mathrm{eq}\right)}\,, \tag{11}$$

where K is the equilibrium (association) constant. Sometimes it is also referred to as the binding affinity. A sense of Eq. 11 is demonstrated in Fig. 1: changes in the association rate influence how fast both the concentration of the complexes and that of the free analyte come to equilibrium. Note that their equilibrium values are not changed, because the equilibrium constant is fixed.

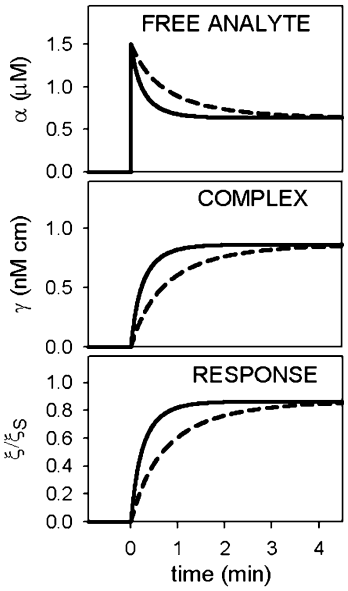

Fig. 1 Analyte-to-receptor binding after the analyte injection, according to the model of the second order reaction in closed volume (Eq. 10). Parameters: $\alpha_0 = 1.5\,\mu\mathrm{M}$, $\beta = 10^{-9}\,\mathrm{M\,cm}$, $S = 1\,\mathrm{cm}^2$, $V = 1\,\mu\mathrm{L}$, $K = 10^7\,\mathrm{M}^{-1}$. *Solid line* $k_\mathrm{a} = 4.5 \times 10^4\,\mathrm{M}^{-1}\,\mathrm{s}^{-1}$, *dashed line* $k_\mathrm{a} = 1.5 \times 10^4\,\mathrm{M}^{-1}\,\mathrm{s}^{-1}$

Very often the number of molecules of analyte in volume V is much higher than the amount of the receptors at the surface S. In this case, the term $\gamma S/V$ in Eq. 10 can be neglected and we obtain:

$$\frac{\mathrm{d}\gamma}{\mathrm{d}t} = k_\mathrm{a}\alpha_0\left(\beta - \gamma\right) - k_\mathrm{d}\gamma\,. \tag{12}$$

Equation 12, originally derived by Langmuir for interactions at a surface in contact with reactants in solution, is formally identical with the equation describing a first-order reaction in solution. It is therefore usually referred to as pseudo first-order kinetics. Its solution is a single exponential function with an asymptote corresponding to the equilibrium fulfilling equation:

$$K = \frac{k_\mathrm{a}}{k_\mathrm{d}} = \frac{\gamma_\mathrm{eq}}{\alpha_0\left(\beta - \gamma_\mathrm{eq}\right)}\,. \tag{13}$$

Pseudo first-order kinetics is also typical for sensors that employ flow cells, where the free analyte concentration is primarily controlled by flowing a solution through the cell. In this case, the free analyte concentration can be either increased stepwise or decreased stepwise. As a result, an SPR sensorgram usually consists of two stages: an association stage that begins with the stepwise increase of the free analyte concentration to a constant value α_0, followed by a dissociation stage where the free analyte concentration is stepped down to zero. An ideal SPR response corresponding to this experiment (pseudo first-order kinetics) is shown in Fig. 2.

After a sufficiently long time, the association and the dissociation rates become practically equal and a dynamic equilibrium state is achieved. The

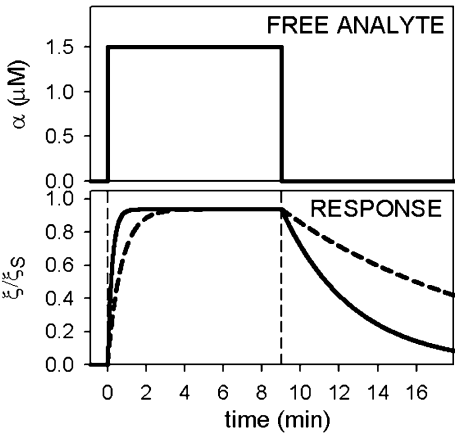

Fig. 2 Ideal flow-cell sensorgram according to the model of pseudo first-order reaction (Eq. 12). Parameters: $\alpha_0 = 1.5\,\mu\mathrm{M}$, $\beta = 1\,\mathrm{nM\,cm}$, $K = 10^7\,\mathrm{M^{-1}}$. *Solid line* $k_\mathrm{a} = 4.5 \times 10^4\,\mathrm{M^{-1}\,s^{-1}}$, *dashed line* $k_\mathrm{a} = 1.5 \times 10^4\,\mathrm{M^{-1}\,s^{-1}}$. *Vertical dashed lines* indicate beginning of the association and the dissociation stage

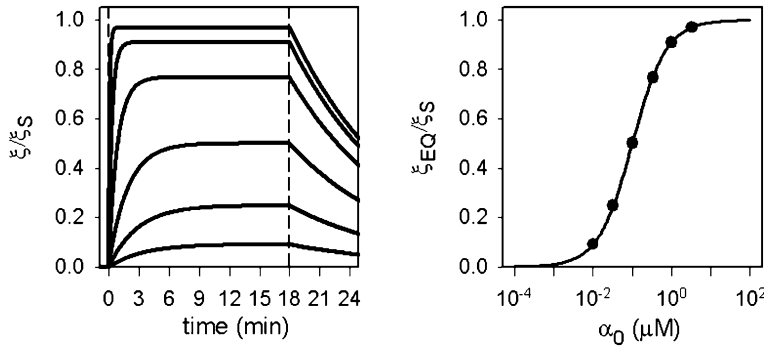

Fig. 3 Set of sensorgrams (model) suitable for equilibrium analysis (*left*) and binding isotherm with indicated equilibrium sensorgram results (*right*). Model of pseudo first-order reaction. Parameters: $\beta = 1$ nM cm, $K = 10^7$ M^{-1}, $k_a = 4.5 \times 10^4$ M^{-1} s^{-1}

equilibrium association constant K [3–7] can be determined by measuring the dependence of the sensor's equilibrium response on the injected analyte concentration (binding isotherm). For pseudo first-order kinetics the binding isotherm (Fig. 3) is given by:

$$\frac{\xi_{EQ}}{\xi_S} = \frac{K\alpha_0}{(1 + K\alpha_0)} . \tag{14}$$

An advantage of equilibrium analysis is that, in contrast to the other parts of the sensorgram, the equilibrium phase of the association curve is not affected by mass transport (see below).

2.2 Other Kinetic Models

In reality, the processes in the active sensor layer may be more complicated and the sensor response will be a superposition of several parallel or consecutive reactions. We will present some kinetic models that correspond to more complex molecular interactions at the sensor surface.

Zero order reactions following the initial binding are usually interpreted as conformational changes of the AR complex. Once the conformation is changed, the complex cannot dissociate unless it transforms back into its original state. This additional reaction can slow down the kinetics. The model, first presented in [8], has been applied in a few studies of complex biomolecular systems where the analyte binding may substantially change the physicochemical properties of the receptor, such as the interaction of angiotensin II with a receptor at a lipid membrane [9] or the interactions of sulfated polysaccharides with immobilized enzyme targets [10]. The reaction scheme of this

two-state model is:

$$\mathrm{A} + \mathrm{R} \underset{k_{\mathrm{d1}}}{\overset{k_{\mathrm{a1}}}{\rightleftharpoons}} \mathrm{AR} \underset{k_{\mathrm{d2}}}{\overset{k_{\mathrm{a2}}}{\rightleftharpoons}} \mathrm{AR}^{*} \,. \tag{15}$$

Assigning γ_1 and γ_2 to the concentrations of the complex in particular states:

$$\gamma_1 = [\mathrm{AR}] \,, \quad \gamma_2 = \left[\mathrm{AR}^{*}\right] \,, \tag{16}$$

the corresponding kinetic equations that account for the relationships between both types of complexes and the free receptor sites can be written as:

$$\begin{aligned} \frac{\partial \gamma_2}{\partial t} &= k_{\mathrm{a2}}\gamma_1 - k_{\mathrm{d2}}\gamma_2 \\ \frac{\partial \gamma_1}{\partial t} &= k_{\mathrm{a1}}\alpha_0 \left(\beta - \gamma_1 - \gamma_2\right) - \frac{\partial \gamma_2}{\partial t} \\ &= k_{\mathrm{a1}}\alpha_0 \left(\beta - \gamma_1 - \gamma_2\right) - k_{\mathrm{d1}}\gamma_1 - k_{\mathrm{a2}}\gamma_1 + k_{\mathrm{d2}}\gamma_2 \,. \end{aligned} \tag{17}$$

As the conformational change does not influence the mass of the complex, the sensor response will be:

$$\xi/\xi_{\mathrm{S}} = \left(\gamma_1 + \gamma_2\right)/\beta \,. \tag{18}$$

Models of parallel pseudo first-order reactions consider the case when two interactions with different rate constants proceed simultaneously. Such situations can be attributed to different kinds of receptor sites or to different states of the analyte [8, 11]. In the first case the model can describe heterogeneity of the sensor surface; the second may concern a macromolecular analyte that can be present in various conformations, protonation states, etc. Besides two sets of rate constants, the models also require specification of proportion p between the two fractions of the receptor or analyte. For the model considering two kinds of receptors, the following equations are obtained:

$$\mathrm{A} + \mathrm{R}_1 \underset{k_{\mathrm{d1}}}{\overset{k_{\mathrm{a1}}}{\rightleftharpoons}} \mathrm{AR}_1 \quad \mathrm{A} + \mathrm{R}_2 \underset{k_{\mathrm{d2}}}{\overset{k_{\mathrm{a2}}}{\rightleftharpoons}} \mathrm{AR}_2 \tag{19}$$

$$\beta_1 = [\mathrm{R}_1] = p\beta \quad \beta_2 = [\mathrm{R}_2] = \left(1 - p\right)\beta \quad \gamma_1 = [\mathrm{AR}_1] \quad \gamma_2 = [\mathrm{AR}_2]$$

$$\frac{\mathrm{d}\gamma_1}{\mathrm{d}t} = k_{\mathrm{a1}}\alpha_0 \left(\beta_1 - \gamma_1\right) - k_{\mathrm{d1}}\gamma_1 \quad \frac{\mathrm{d}\gamma_2}{\mathrm{d}t} = k_{\mathrm{a2}}\alpha_0 \left(\beta_2 - \gamma_2\right) - k_{\mathrm{d2}}\gamma_2 \tag{20}$$

$$\xi/\xi_{\mathrm{S}} = \left(\gamma_1 + \gamma_2\right)/\beta \,.$$

Results of this model are illustrated in Fig. 4. For the case with two states of the analyte, the equations are analogous to the previous ones except that the

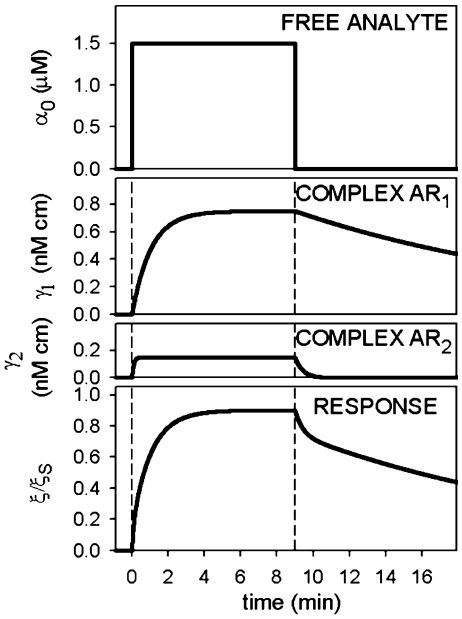

Fig. 4 Kinetics and sensorgram according to the model of two parallel pseudo first-order reactions attributed to two kinds of receptors (Eq. 19). Parameters: $\alpha_0 = 1.5\ \mu M$, $\beta = 1\ nM\ cm$, $p = 0.8$, $k_{a1} = 10^4\ M^{-1}\ s^{-1}$, $k_{d1} = 0.001\ s^{-1}$, $k_{a2} = 8 \times 10^4\ M^{-1}\ s^{-1}$, $k_{d2} = 0.04\ s^{-1}$

effect of competition for the receptor sites must be included:

$$A_1 + R \underset{k_{d1}}{\overset{k_{a1}}{\rightleftharpoons}} A_1R \quad A_2 + R \underset{k_{d2}}{\overset{k_{a2}}{\rightleftharpoons}} A_2R \tag{21}$$

$$\alpha_1 = [A_1] = p\alpha_0 \quad \alpha_2 = [A_2] = (1-p)\,\alpha_0 \quad \gamma_1 = [A_1R] \quad \gamma_2 = [A_2R]$$

$$\frac{d\gamma_1}{dt} = k_{a1}\alpha_1\left(\beta - \gamma_1 - \gamma_2\right) - k_{d1}\gamma_1 \quad \frac{d\gamma_2}{dt} = k_{a2}\alpha_2\left(\beta - \gamma_1 - \gamma_2\right) - k_{d2}\gamma_2 \tag{22}$$

$$\xi/\xi_S = \left(\gamma_1 + \gamma_2\right)/\beta\,.$$

Equations 22 can also be employed in the case of two different analytes, although the last relationship for calculating the sensor response must be modified to account for the different masses of the analytes.

Multivalent receptor binding is a case when a single receptor molecule can bind more than one molecule of analyte. Multivalent binding capacity is a frequent feature of many biomolecular systems, for instance antibodies. Another example is the formation of triplexes by oligonucleotides. If a purine oligonucleotide is fixed at the sensor surface as a receptor, a complementary oligonucleotide can bind to it and to create a duplex. In special cases, another oligonucleotide molecule may bind to the duplex and form a triplex.

This situation involves two successive reactions, each occurring at a unique binding site. The corresponding kinetic equations are:

$$\mathrm{A} + \mathrm{R} \underset{k_{\mathrm{d1}}}{\overset{k_{\mathrm{a1}}}{\rightleftharpoons}} \mathrm{AR} \quad \mathrm{AR} + \mathrm{A} \underset{k_{\mathrm{d2}}}{\overset{k_{\mathrm{a2}}}{\rightleftharpoons}} \mathrm{ARA} \tag{23}$$

$$\gamma_1 = [\mathrm{AR}] \quad \gamma_2 = [\mathrm{ARA}]$$

$$\frac{\partial \gamma_2}{\partial t} = k_{\mathrm{a2}} \alpha_0 \gamma_1 - k_{\mathrm{d2}} \gamma_2 \tag{24}$$

$$\begin{aligned} \frac{\partial \gamma_1}{\partial t} &= k_{\mathrm{a1}} \alpha_0 \left(\beta - \gamma_1 - \gamma_2\right) - k_{\mathrm{d1}} \gamma_1 - \frac{\partial \gamma_2}{\partial t} \\ &= k_{\mathrm{a1}} \alpha_0 \left(\beta - \gamma_1 - \gamma_2\right) - k_{\mathrm{d1}} \gamma_1 - k_{\mathrm{a2}} \alpha_0 \gamma_1 + k_{\mathrm{d2}} \gamma_2 \end{aligned}$$

$$\xi / \xi_{\mathrm{S}} = \left(\gamma_1 + 2\gamma_2\right) / \beta \, .$$

Here the standard sensor response is assumed to be the case when all receptors are bound in 1 : 1 complexes (duplexes). That is why the relative response can exceed 1, as is seen in Fig. 5.

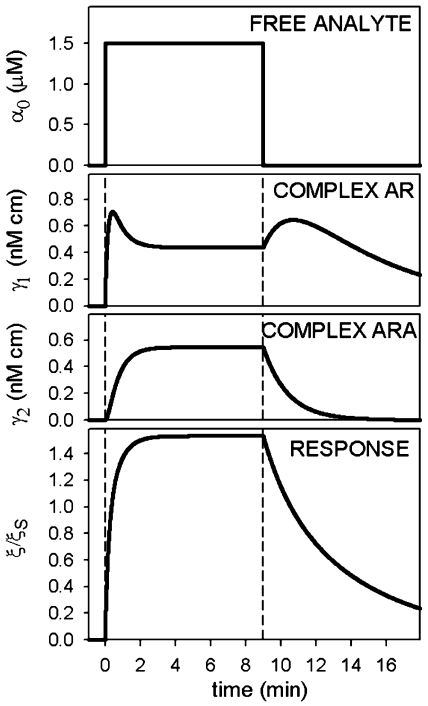

Fig. 5 Kinetics and sensorgram according to the model of consecutive two binding reactions in case of bivalent receptor (Eq. 23). Parameters: $\alpha_0 = 1.5$ μM, $\beta = 1$ nM cm, $k_{\mathrm{a1}} = 6 \times 10^4$ M^{-1} s^{-1}, $k_{\mathrm{d1}} = 0.003$ s^{-1}, $k_{\mathrm{a2}} = 10^4$ M^{-1} s^{-1}, $k_{\mathrm{d2}} = 0.012$ s^{-1}

Binding of a multivalent analyte occurs when a single analyte molecule can simultaneously occupy more than one receptor molecule. This case does not mirror the previous one, because the resulting analyte/receptor interaction strongly depends on the receptor distribution on the sensor surface. For sufficiently sparse receptor spacing, only a single binding mode is available despite the number of analyte binding sites – once the analyte is caught by a receptor, it is isolated from other distant receptors. Increasing the receptor density increases the probability of forming a receptor pattern that allows an analyte to bind multiple receptors. In [12] the authors introduced the concept of dividing the active sensor layer into spheres with a radius equal to the functional distance between the two binding sites of the analyte. Using Poisson statistics they estimated the portion p of those receptors (R_C) that were at least by two inside one sphere. Remaining receptors (R_S) were expected to be single within a sphere. The kinetic model considered simple 1 : 1 binding on R_S receptors and consecutive binding on R_C receptors:

$$A + R_S \underset{k_d}{\overset{k_a}{\rightleftharpoons}} AR_S \quad A + R_C \underset{k_d}{\overset{k_a}{\rightleftharpoons}} AR_C \quad AR_C + R_C \underset{k_d}{\overset{k_a}{\rightleftharpoons}} AR_CR_C\,. \tag{25}$$

Assuming the same rate constants for both binding sites on the analyte, the following set of equations is obtained:

$$\begin{aligned}
&\beta_1 = [R_S] = (1-p)\,\beta \quad \beta_2 = [R_C] = p\beta \\
&\gamma_1 = [AR_S] \quad \gamma_2 = [AR_C] \quad \gamma_3 = [AR_CR_C] \\
&\frac{\partial\gamma_1}{\partial t} = 2k_a\alpha_0\left(\beta_1 - \gamma_1\right) - k_d\gamma_1 \quad \frac{\partial\gamma_2}{\partial t} = 2k_a\alpha_0\left(\beta_2 - \gamma_2 - 2\gamma_3\right) - k_d\gamma_2 - \frac{\partial\gamma_3}{\partial t} \\
&\frac{\partial\gamma_3}{\partial t} = k_a\gamma_2\frac{\beta_2 - \gamma_2 - 2\gamma_3}{\beta_2}\frac{1}{V_{sp}N_A} - 2k_d\gamma_3 \\
&\xi/\xi_S = \left(\gamma_1 + \gamma_2 + 2\gamma_3\right)/\beta\,.
\end{aligned} \tag{26}$$

Note that a factor of 2 appears in the kinetic equations to account for the doubled probability because of two binding sites on the analyte. In the equation for $\frac{\partial\gamma_3}{\partial t}$, the fraction $\frac{\beta_2-\gamma_2-2\gamma_3}{\beta_2}$ is the probability that there is a free receptor inside the sphere where the AR_C complex occurs. The second fraction, $\frac{1}{V_{sp}N_A}$, where V_{sp} is the sphere volume and N_A is Avogadro's number, represents the concentration of the available analyte – one molecule in the V_{sp} sphere. It has been demonstrated in [12] that this model fits experimental data substantially better than a solvent kinetic model of multiple binding, which does not respect the fixed positions of the receptors.

At the end of this section it is worth mentioning that besides SPR studies where the analyte binding to the receptor is the only running interaction, competitive SPR biosensor experiments with two concurrent interactions,

i.e., analyte-immobilized receptor and analyte-another ligand in solution, can also be performed. Proper kinetic models for competitive SPR studies should be developed based on the appropriate kinetic equations for the particular interactions, using an approach analogous to the aforementioned cases.

2.3 Thermodynamic Context of Equilibrium and Kinetic Constants

The equilibrium association constant K is directly related to the change of the molar Gibbs energy attributed to complex formation ΔG^0:

$$\Delta G^0 = -RT \ln \left(K_a C^0 \right) , \tag{27}$$

where R is the universal gas constant, T is the absolute temperature, and C^0 is a standard concentration – as a rule its value is taken as 1 M. The basic temperature dependence of ΔG is given by the van't Hoff equation:

$$\Delta G = \Delta H - T\Delta S , \tag{28}$$

where ΔH and ΔS are the changes of enthalpy and of entropy. If they are both temperature independent, a plot of $\ln \left(K_a C^0 \right)$ versus $1/T$ (van't Hoff plot) should be linear. The ΔH and ΔS values can be determined directly from the graph; more precise is a least square fit of Eqs. 27 and 28.

The simple van't Hoff equation (Eq. 28) is not completely correct if the complex formation results in a change of the specific heat capacity ΔC_p, in which case neither ΔH nor ΔS are exactly independent of temperature. A more precise form of the van't Hoff equation is [13]:

$$\Delta G\left(T\right) = \Delta H_{To} - T\Delta S_{To} + \Delta C_p \left(T - T_0\right) + \Delta C_p T \ln \left(\frac{T}{T_0} \right) , \tag{29}$$

where T_0 is a reference temperature. To obtain reliable values of ΔH_{To}, ΔS_{To}, and ΔC_p (T_0 is defined, usually $T_0 = 298.15$ K, i.e., 25 °C), precise data over a wider range of temperatures are necessary for the fit. Estimation of any of the thermodynamic parameters from another experiment is very helpful.

The temperature dependence of k_a and k_d is usually characterized by means of activation energy (E_a^{act} and E_d^{act}) according to the Arrhenius equation:

$$\ln k = \ln P - \frac{E^{act}}{RT} , \tag{30}$$

where P is a constant known as the pre-exponential factor. The activation energy is assumed to be a measure of the amount of thermal energy required for binding or dissociation. Because E_a^{act} and E_d^{act} can be considered as activation enthalpies, the reaction enthalpy can be calculated from the relationship:

$$\Delta H = E_a^{act} - E_d^{act} . \tag{31}$$

An unusually high E^{act} value indicates that binding and/or dissociation requires the surmounting of high potential energy barriers, suggesting that conformational rearrangements are required.

When possible, the kinetic rate constants determined using SPR sensors have been compared to those obtained in bulk solution using other methods. Good agreement was obtained only in some cases. For instance, it has been reported [14] that when a study of the interactions between small inhibitor molecules and immobilized proteins was carefully designed, performed, and analyzed, very good agreement with the bulk data was achieved.

The basic formula for the association rate constant is given by Debye–Smoluchowski theory:

$$k_a = 4\pi\varphi\varepsilon r \left(D_A + D_R\right) N_A/1000 \,, \tag{32}$$

where φ is a steric interaction factor, ε is an electrostatic interaction factor, r is an interaction radius. D_A and D_R are translation diffusion coefficients of the analyte and the receptor molecule.

Let us consider the term of the translation diffusion. The diffusion coefficient D expresses the ability of a molecule to change its position in solution due to chaotic translation motion. Basic evaluation of the diffusion coefficient can be obtained from the Stokes formula for a sphere in a fluid:

$$D = \frac{k_B T}{6\pi a \eta} \,, \tag{33}$$

where k_B is the Boltzmann constant, T is the absolute temperature, η is the viscosity of the fluid and a is the radius of the sphere approximating the molecule size. Therefore, the diffusion coefficient decreases strongly with increasing size of the molecule. In contrast to the case of both interaction partners in solution, the translation diffusion of the receptor is limited when it is immobilized at the sensor surface. The value inside the parentheses in Eq. 32 may then be reduced and approximated as close to the D_A term alone. The final effect of immobilization on the translation diffusion term would depend on the ratio between D_A and D_R. If the receptor is a large molecule like protein and the analyte is a small molecule like the inhibitors used in the experiments reported in [14], then $D_A \approx (D_A + D_R)$ and the association and dissociation rate constants may be very close for both the SPR biosensor and for reactions in the bulk. On the other hand, a small receptor interacting with a large analyte may be characterized by rate constants significantly different from those measured in the bulk.

To conclude this section we summarize that, in general, the kinetic rate constants obtained from SPR sensors may not agree with those obtained in solution. The SPR technique seems to be better suited to performing comparative studies of molecules according their affinity and other interaction characteristics. However, improvements in the precision of SPR measurements and of their theoretical description may soon lead to new approaches for ex-

tracting fundamental information about biomolecular interactions using SPR sensors with receptors with varying degrees of restricted mobility.

3 Mass Transport Effects

In SPR biosensors, the rate of biomolecular interactions at the surface depends on the free analyte transport toward (association stage) or away from (dissociation stage) the active zone. The stepwise free analyte concentration changes discussed above are only an idealization, because the free analyte transport is always limited. The influence of analyte transport on the reactions at the sensor surface is given by comparing the transport throughput to the kinetic rates. Slow analyte transport causes a decrease in its concentration when it is consumed during the association phase and an increase when it is produced during the dissociation phase. As a result, both reactions are slowed down.

This effect is illustrated in Fig. 6 where the kinetics of a simple pseudo first-order reaction are calculated assuming that analyte transport is propor-

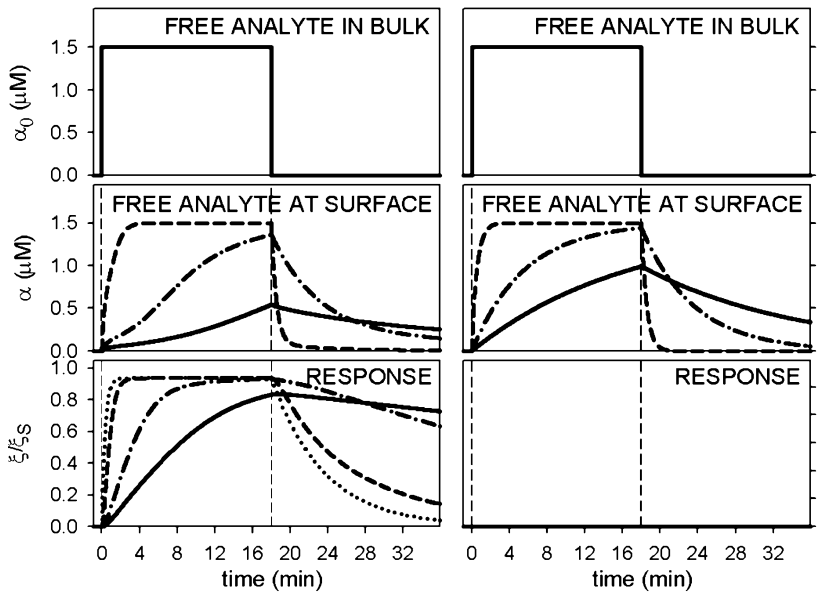

Fig. 6 Free analyte concentrations in the active layer and sensorgrams for the pseudo first-order reaction and two-compartment model of the analyte transport. Parameters: α_0 = 1.5 μM, β = 1 nM cm. *Left* $k_a = 0.03\ M^{-1}\ s^{-1}$, $k_d = 0.003\ s^{-1}$; *right* no binding of analyte to receptor. Rate constant of the analyte diffusion flux (Eq. 32) $k_M/h_{layer} = 3 \times 10^{-5}\ s^{-1}\ cm^{-1}$ (*dashed line*), $3 \times 10^{-6}\ s^{-1}\ cm^{-1}$ (*dash-and-dot*), and $10^{-6}\ s^{-1}\ cm^{-1}$ (*solid*). *Dotted line* no limitations of the analyte transport

tional to the concentration difference between the bulk analyte solution and the active sensor layer (two-compartment model, discussed in greater detail later). In addition to the effect on analyte binding kinetics, the figure also clearly illustrates that the reaction between the receptor and analyte influences, i.e., significantly reduces the free analyte concentration. If the reaction does not occur (right-hand figures), the free analyte concentration reaches its equilibrium value more rapidly.

3.1 Analyte Transport in a Flow Cell

The flow cell shape is typically rectangular with its length l (dimension along the flow) and width w (dimension perpendicular to the flow and parallel to the sensor surface) in the range 10^{-0}–10^{-2} cm, and a substantially lower height h (dimension perpendicular to the sensor surface) measuring 10^{-2}–10^{-3} cm. Flow characteristics can be described by the Reynolds number:

$$\mathrm{Re} = \frac{\rho \Phi}{\eta h}\,, \tag{34}$$

where ρ and η are the density and viscosity of the fluid, and Φ is the flow rate (volume of fluid passing through the cell per unit time interval). The flow is expected to be laminar (without turbulence) if $\mathrm{Re} < 2100$ [15]. For water at 20 °C, $\mathrm{Re} = (\Phi/h) \cdot 0.998\ \mathrm{mm^2\ s^{-1}}$. Considering typical flow cell dimensions and flow rates, the Reynolds number does not exceed several hundreds. The distance between the active sensor surface and both the inlet and outlet is as a rule far enough that the laminar flow profile is fully developed in the active sensor region [16]. The velocity profile is therefore considered as constant over the sensor active zone.

Let us introduce spatial coordinates in the flow-cell interior: x in direction of the length, y in direction of the height, and z in direction of the width. The magnitude of the velocity (its direction is uniformly parallel to the x-axis) depends mainly on y. The velocity profile is parabolic, with the maximum velocity $v_{\max}$ at the mid-point of the cell height and zero velocity at the cell walls. In contrast, the velocity dependence on z is negligible (except for the regions very close to the cell walls, which are sufficiently far from the active region) [17]. The total fluid flux through the flow cell can thus be obtained by integrating over the y coordinate from zero to h. This provides a relation between $v_{\max}$, the cell dimensions, and Φ:

$$v_{\max} = \frac{3}{2}\frac{\Phi}{hw}\,. \tag{35}$$

Similarly to the flow velocity, other parameters characterizing analyte transport are also constant in the z-direction. This allows us to reduce the transport problem to two spatial dimensions described by the coordinates x and y.

The actual analyte concentration, which is of course no longer constant, is then described as a function of these two coordinates, $\alpha = \alpha\left(x, y, t\right)$. The time dependence of the analyte concentration is given by the continuity equation. If no transport mechanism other than the laminar flow is considered, a partial differential equation is obtained:

$$\frac{\partial\alpha\left(x,y,t\right)}{\partial t} = -\,v\left(y\right)\frac{\partial\alpha\left(x,y,t\right)}{\partial x} = -\,4v_{\max}\frac{y}{h}\left(1-\frac{y}{h}\right)\frac{\partial\alpha\left(x,y,t\right)}{\partial x}\,. \tag{36}$$

To model the effect of an analyte injection, the equation has to be solved for an initial condition of zero analyte concentration inside the flow cell at $t = 0$ and a boundary condition of analyte concentration α_0 at the entrance of the flow cell $\alpha\left(0, y, t\right) = \alpha_0$. Results are shown in Fig. 7. It can be seen that for the central part of the vertical profile the injected analyte concentration α_0 is achieved relatively rapidly (depending on the flow rate), but the analyte concentrations remains zero in close proximity of the cell walls. This is a direct consequence of laminar flow – analyte transport to the active surface layer by laminar flow alone is very ineffective.

The other transport mechanism, i.e., translational diffusion of the analyte, becomes therefore highly important in the vicinity of the active sensor layer. Translational diffusion is a mechanism that leads to concentration uniformity in non-mixed solutions. It is described by the first Fick's law that states proportionality between the rate of diffusion and the concentration gradient.

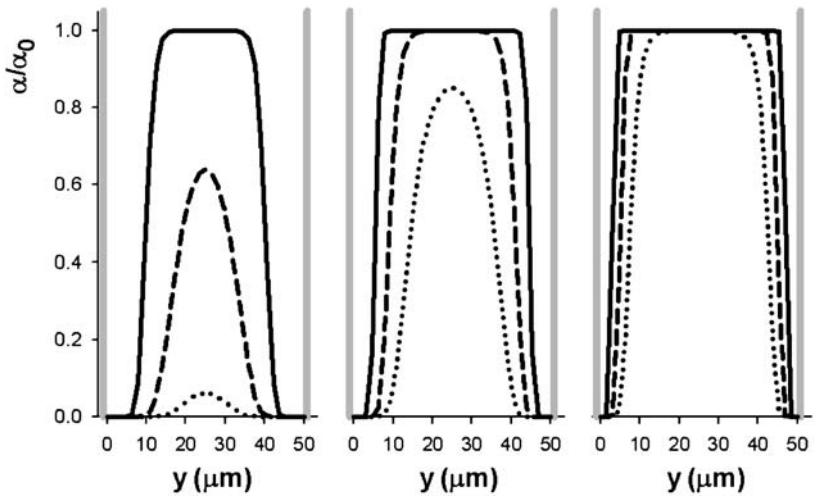

Fig. 7 Analyte concentration in a flow cell at 10 mm distance from the injection entrance reached 3 s (*dotted line*), 6 s (*dashed*), and 15 s (*solid*) after beginning of the injection as a consequence of pure laminar flow (diffusion not considered). Flow rates were 10 μL min^{-1} (*left*), 30 μL min^{-1} (*middle*), and 90 μL min^{-1} (*right*). Cell dimensions: 20 mm (length) × 2.7 mm (width) × 0.05 mm (height)

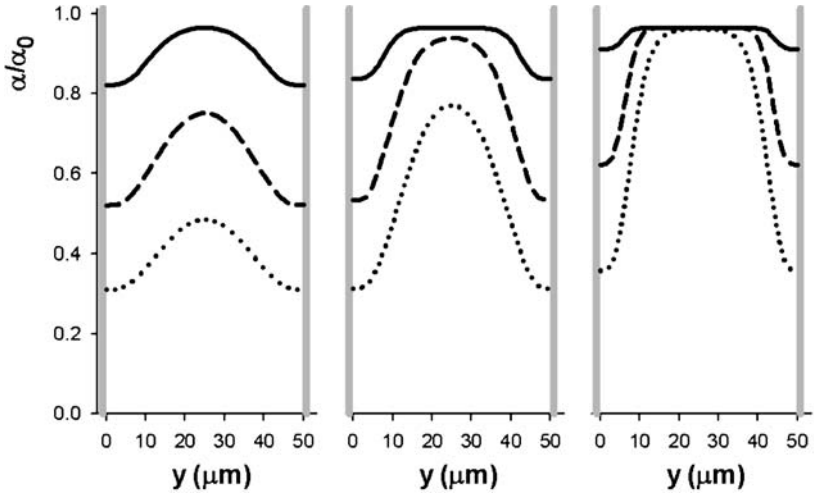

Fig. 8 Analyte concentration in a flow cell at 10 mm distance from the injection entrance reached 3 s (*dotted line*), 6 s (*dashed*), and 15 s (*solid*) after beginning of the injection as a consequence of laminar flow and diffusion. Flow rates were 10 μL min^{-1} (*left*), 30 μL min^{-1} (*middle*), and 90 μL min^{-1} (*right*), diffusion coefficient 10^{-6} cm^2 s^{-1}. Cell dimensions: 20 mm (length) × 2.7 mm (width) × 0.05 mm (height)

The proportionality constant D is called the diffusion coefficient and quantifies the chaotic translation motion of the molecules in solution. Its basic evaluation is given by the Stokes formula (Eq. 33). The diffusion coefficient decreases as the size of the molecule increases. For typical biomolecules in aqueous medium, D is usually between 10^{-7} cm^2 s^{-1} and 10^{-6} cm^2 s^{-1}. Temperature dependence of the diffusion coefficient follows T/η, where T is absolute temperature and η viscosity of the solvent, unless the temperature change does not alter the molecular shape.

If the translation diffusion is taken into account, the equation of the analyte transport will become:

$$\frac{\partial \alpha\left(x,y,t\right)}{\partial t} = D\left(\frac{\partial^2 \alpha\left(x,y,t\right)}{\partial x^2} + \frac{\partial^2 \alpha\left(x,y,t\right)}{\partial y^2}\right) - 4v_{\max}\frac{y}{h}\left(1-\frac{y}{h}\right)\frac{\partial \alpha\left(x,y,t\right)}{\partial x}. \tag{37}$$

The effect of diffusion on the analyte distribution is shown in Fig. 8, where Eq. 37 was solved using the same boundary conditions that were applied to Eq. 35 to generate Fig. 7. Note the significant increase in analyte concentration near the cell walls, thanks to diffusion.

3.2
Full Model of Mass Transport

A rigorous approach to modeling the reaction kinetics at the sensor surface, including the mass transport effects, requires solving the fundamental par-

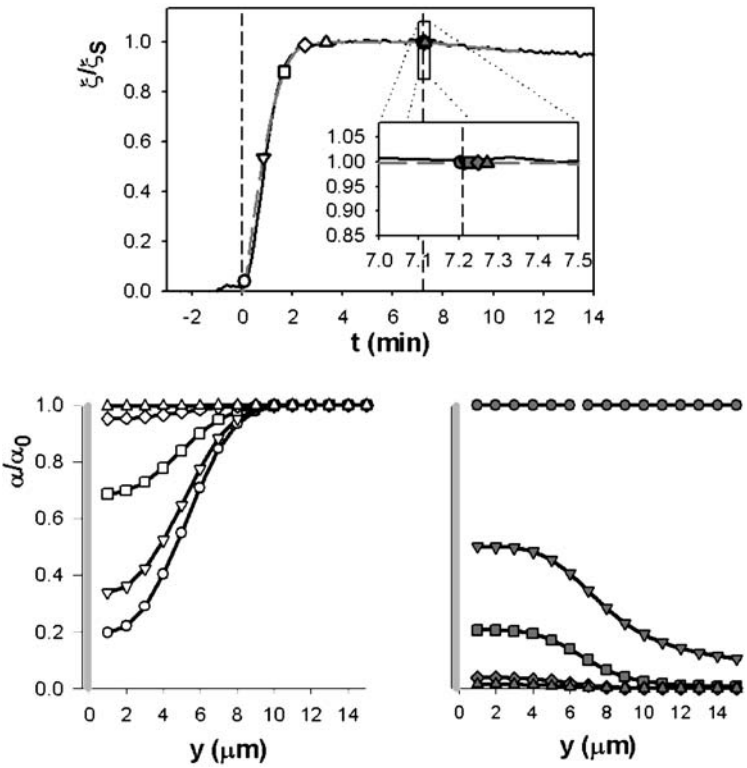

Fig. 9 Results of the full model of the analyte transport coupled to pseudo first-order reaction kinetics. The model fitted to experimental sensorgram of DNA 23-mer binding to its immobilized complementary DNA chain. The experimental sensorgram (*upper graph, black solid line* with the association and dissociation periods indicated by *vertical dashed lines*) is very well fitted by the theoretical course of the relative sensor response (*gray long dashes*). The *graphs below* show the free analyte concentration in the close vicinity of the active sensor layer as it is distributed 6, 50, 100, 150, and 200 s after the injection (on the *left*, from the *bottom up*) and 0, 0.5, 1.12, 2.4, and 3.75 s after stopping the injection (on the *right*, from the *top down*). The times corresponding to particular concentration profiles are indicated in the *upper graph* by same *graphical symbols*. In the case of the dissociation phase they can be resolved only after expansion of the time axis (*insert*). Parameters: $\alpha_0 = 10^{-7}$ M, $\beta = 1.84 \times 10^{-9}$ M cm, $\Phi = 70\,\mu$L min^{-1}, $D = 2.5 \times 10^{-6}$ cm^2 s^{-1}, $k_a = 5.6 \times 10^5$ M^{-1} s^{-1}, $k_d = 2.5 \times 10^{-6}$ s^{-1}. The model was applied to the central part of the flow cell (*xy* coordinates corresponding to the active zone of the sensor) with dimensions of 2.5 mm × 2.7 mm × 0.04 mm

tial differential (Eq. 37, PDE) coupled with the relevant kinetic equations. The coupling is twofold. First, we have to apply the actual analyte concentration at the given point on the sensor surface. As this value varies along the x-coordinate, the concentration of analyte/receptor complexes can no longer be considered as only time dependent – it must be described as a function of t and x: $\gamma = \gamma(x, t)$. The kinetic equations need to be modified accordingly; for instance, the equation of simple first-order kinetics (Eq. 12) is modified as follows:

$$\frac{\mathrm{d}\gamma(x,t)}{\mathrm{d}t} = k_\mathrm{a}\alpha(x,0,t)\,[\beta - \gamma(x,t)] - k_\mathrm{d}\gamma(x,t)\,. \tag{38}$$

Secondly, we have to introduce the consumption or production of the free analyte due to the interaction with receptors to the PDE. It is usually performed [18–20] via a specific boundary condition that in the case of single reaction kinetics is:

$$D\frac{\partial\alpha(x,0,t)}{\partial y} = \frac{\partial\gamma(x,t)}{\partial t}\,. \tag{39}$$

For more complex reaction kinetics the right side of the equation must comprise all kinds of complexes (the formation of which requires consumption of the analyte) multiplied by respective stoichiometric factors. Analogously to Eq. 39, a boundary condition of:

$$\frac{\partial\alpha(x,h,t)}{\partial y} = 0 \tag{40}$$

is introduced for the flow-cell wall opposite to the sensor surface.

Equation 37 can be solved only numerically. Most often a finite element method with various grids in the xy region of the flow cell is employed [18], but other approaches have also been tested [19]. An illustration of the full model results is given in Fig. 9.

The enormously time-consuming nature of full model calculations prevents this approach from being used for complete fits of experimental data. As a rule, it is employed to verify simpler models and/or to confirm the reasonability of rate constants by comparison with experimental data. To enable more convenient and routine analysis of measured sensorgrams, simpler models of mass transport effects have been derived.

3.3
Simplified Models of Mass Transport

The first simplification of Eq. 37 is based on the assumption that the analyte transport in the x direction is mainly conductive, i.e., it is controlled by the flow in the cell. The relation between conductive transport and diffusion in y direction is often characterized by the Peclét number, which reflects the ratio of the ideal time required for an analyte molecule to diffuse from the cell

middle ($y = h/2$) to the cell wall, to the minimal time required for that same molecule to pass through the cell by the laminar flow:

$$\mathrm{Pe} = \frac{v_{\max} h^2}{Dl} \,. \tag{41}$$

If the Peclét number is high compared to 1 ($\mathrm{Pe} \gg 1$), Eq. 37 can be simplified by omitting the diffusion term in the x direction and by linearizing the flow velocity dependence on y, because we can limit calculations of the analyte concentration to a region close to the sensor surface ($y \ll h$) [20–22]. We find:

$$\frac{\partial \alpha\left(x,y,t\right)}{\partial t} = D\frac{\partial^2 \alpha\left(x,y,t\right)}{\partial y^2} - 4v_{\max}\frac{y}{h}\frac{\partial \alpha\left(x,y,t\right)}{\partial x} \,. \tag{42}$$

For a pseudo first-order analyte-to-receptor reaction this equation coupled with the reaction kinetics Eq. 38 via Eq. 39 can be solved so that an equation for only $\gamma(x,t)$ is obtained:

$$\begin{aligned}\frac{\partial \gamma(x,t)}{\partial t} = {} & k_{\mathrm{a}}\alpha_0\left[\beta - \gamma(x,t)\right] \\ & \times\left[1 - \frac{Fh}{\alpha_0 Dl\mathrm{Pe}^{1/3}}\int_0^x \frac{\partial \gamma(u,t)}{\partial t}(x-u)^{2/3}\mathrm{d}u\right] - k_{\mathrm{d}}\gamma(x,t)\end{aligned} \tag{43}$$

$$F = \frac{1}{12^{1/3}\Gamma(2/3)} \approx 0.32256 \,.$$

Equation 43, which is much easier to solve than the full model, can be further simplified in order to eliminate the integral term. This approximation can be applied when the dependence of $\frac{\partial \gamma(x,t)}{\partial t}$ on x is rather weak and can be assumed to be linear. This linearization allows the integral term to be evaluated explicitly. The result can be written formally in a form analogous to the original kinetic equation (Eq. 12):

$$\frac{\mathrm{d}\gamma(x,t)}{\mathrm{d}t} = k_{\mathrm{a}}^{\mathrm{ef}}(x,t)\alpha_0\left[\beta - \gamma(x,t)\right] - k_{\mathrm{d}}^{\mathrm{ef}}(x,t)\gamma(x,t) \,, \tag{44}$$

where the "effective" rate constants, however, are both space- and time-dependent:

$$k_{\mathrm{a}}^{\mathrm{ef}} = \frac{k_{\mathrm{a}}}{1 + k_{\mathrm{a}}\left[\beta - \gamma(x,t)\right]/k_{\mathrm{M}}(x)} \qquad k_{\mathrm{d}}^{\mathrm{ef}} = \frac{k_{\mathrm{d}}}{1 + k_{\mathrm{a}}\left[\beta - \gamma(x,t)\right]/k_{\mathrm{M}}(x)} \tag{45}$$

$$k_{\mathrm{M}}(x) \approx 1.034\left(\frac{v_{\max}D^2}{hx}\right)^{1/3} \,.$$

Thanks to the previously applied assumption that $\gamma(x,t)$ is linearly dependent on x, it is also possible to integrate it over the active sensor region. As a result, we obtain equations analogous to Eq. 44, where $\gamma(x,t)$ is replaced by the

average concentration of complexes $\langle\gamma\rangle(t)$:

$$\frac{\mathrm{d}\langle\gamma\rangle(t)}{\mathrm{d}t} = k_\mathrm{a}^\mathrm{ef}(t)\alpha_0\left[\beta - \langle\gamma\rangle(t)\right] - k_\mathrm{d}^\mathrm{ef}(t)\langle\gamma\rangle(t)$$
$$k_\mathrm{a}^\mathrm{ef} = \frac{k_\mathrm{a}}{1 + k_\mathrm{a}\left[\beta - \langle\gamma\rangle(t)\right]/k_\mathrm{M}} \quad k_\mathrm{d}^\mathrm{ef} = \frac{k_\mathrm{d}}{1 + k_\mathrm{a}\left[\beta - \langle\gamma\rangle(t)\right]/k_\mathrm{M}} \tag{46}$$
$$k_\mathrm{M} \approx 1.378\left(\frac{\nu_\mathrm{max}D^2}{hl}\right)^{1/3}.$$

Equations 46 have been directly derived from the full model in [19]. On the other hand, they are almost identical with the relations obtained from the so-called two-compartment model (the only difference is that the numerical coefficient k_M is a little bit lower). The two-compartment model was first developed for sensors with receptors placed on small spheres [23]. In [24–26] it was adapted for the SPR flow cell and in [18] it was approved and verified by comparison of numerical results with those obtained from the full model. The two-compartment model approximates the analyte distribution in the vicinity of the receptors by considering two distinct regions. The first is a thin layer around the active receptor zone of effective thickness h_layer, and the second is the remaining volume with the analyte concentration equal to the injected one, i.e., α_0. While the analyte concentration in the bulk is constant (within a given compartment), analyte transport to the inner compartment is controlled by diffusion. The actual analyte concentration at the sensor surface is then given by the difference between the diffusion flow and the consumption/production of the analyte via interaction with receptors. For the simple pseudo first-order interaction model we obtain:

$$\frac{\mathrm{d}\alpha}{\mathrm{d}t} = \frac{1}{h_\mathrm{layer}}\left[k_\mathrm{M}\left(\alpha_0 - \alpha\right) - \frac{\mathrm{d}\gamma}{\mathrm{d}t}\right]. \tag{47}$$

The constant k_M can be approximated as [22, 27]:

$$k_\mathrm{M} \approx 1.282\left(\frac{\nu_\mathrm{max}D^2}{hl}\right)^{1/3}. \tag{48}$$

For a quasi-steady-state approximation where $\frac{\mathrm{d}\alpha}{\mathrm{d}t}$ is set to zero in Eq. 47, equations analogous to Eq. 46 are obtained from Eqs. 12 and 47.

The k_M value can be considered as a measure of the mass transport. Its effect on the SPR response can be evaluated by the maximal difference of the denominator in Eq. 46 from unity [16]. It is equal to the ratio of the reaction velocity to the diffusion flux of the analyte at the beginning of the association stage:

$$\mathrm{denom.}_\mathrm{max} - 1 = \frac{k_\mathrm{a}\beta}{k_\mathrm{M}} \approx 0.780 \qquad k_\mathrm{a}\beta\left(\frac{\nu_\mathrm{max}D^2}{hl}\right)^{-1/3}. \tag{49}$$

This ratio (excluding the numerical constants) is called Damköhler number (Da):

$$\mathrm{Da} = k_\mathrm{a}\beta\left(\frac{v_\mathrm{max}D^2}{hl}\right)^{-1/3} = \frac{k_\mathrm{a}\beta h}{D\sqrt[3]{\mathrm{Pe}}}\,. \tag{50}$$

For small Damköhler numbers (Da $\ll$ 1) the mass transport is much faster than the surface reaction itself and therefore the mass transport effect may be ignored. On the other hand, if the Damköhler number is high (Da $\gg$ 1) the sensorgram profile is completely controlled by the diffusion mass transfer and is it not possible to determine rate constants of the surface reaction.

All of the transport models presented so far assume that the diffusion mobility of the analyte in the active sensor zone is the same as in the bulk. In case of the sensors using a thick skeleton to fix the receptors, such as a dextran matrix, solgel, or MIPs, it might be useful to take into account varying analyte diffusion mobility inside the active sensor layer. Detail analysis and proposed models can be found in [28].

4 Summary

A constant and homogeneous concentration of free analyte represents the ideal condition for modeling molecular interactions at the surface of an SPR biosensor. In the most frequent case where an analyte binds to an immobilized receptor with 1 : 1 stoichiometry, the interaction follows the pseudo first-order kinetic model. Adequate interaction models can be built up to describe more complex molecular interactions; some of them have been presented and explained above.

The effect of mass transport on molecular binding in the SPR sensor active layer can be evaluated by means of the Damköhler number (Eq. 50). Except for cases of a very low Damköhler number, mass transport has to be regarded in theoretical models by means of the aforementioned equations.

References

1. Ward LD, Winzor DJ (2000) Anal Biochem 285:179
2. de Mol NJ, Plomp E, Fischer MJE, Ruijtenbeek R (2000) Anal Biochem 279:61
3. Fisher RD, Wang B, Alam SL, Higginson DS, Robinson H, Sundquist WI, Hill CP (2003) J Biol Chem 278:28976
4. McDonnell JM (2001) Curr Opin Chem Biol 5:572
5. Oshannessy DJ, Brighamburke M, Soneson KK, Hensley P, Brooks I (1993) Anal Biochem 212:457
6. Rich RL, Myszka DG (2005) J Mol Recog 18:431
7. Rich RL, Myszka DG (2005) J Mol Recog 18:1

8. Morton TA, Myszka DG (1998) Methods Enzymol: Energetics of biological macromolecules. Pt B 295:268
9. Kamimori H, Unabia S, Thomas WG, Aguilar MI (2005) Anal Sci 21:171
10. Shen BJ, Shimmon S, Smith MM, Ghosh P (2003) J Pharm Biomed Anal 31:83
11. Karlsson R, Falt A (1997) J Immunol Methods 200:121
12. Muller KM, Arndt KM, Pluckthun A (1998) Anal Biochem 261:149
13. Yoo SH, Lewis MS (1995) Biochemistry 34:632
14. Day YSN, Baird CL, Rich RL, Myszka DG (2002) Protein Sci 11:1017
15. Bird RB, Stewart WE, Lightfoot EE (2002) Transport phenomena. Wiley, New York
16. Edwards DA (2000) Stud Appl Math 105:1
17. Brody JP, Yager P, Goldstein RE, Austin RH (1996) Biophys J 71:3430
18. Myszka DG, He X, Dembo M, Morton TA, Goldstein B (1998) Biophys J 75:583
19. Mason T, Pineda AR, Wofsy C, Goldstein B (1999) Math Biosci 159:123
20. Edwards DA (1999) IMA J Appl Math 63:89
21. Edwards DA, Goldstein B, Cohen DS (1999) J Math Biol 39:533
22. Lok BK, Cheng YL, Robertson CR (1983) J Colloid Interface Sci 91:104
23. Glaser RW (1993) Anal Biochem 213:152
24. Myszka DG, Morton TA, Doyle ML, Chaiken IM (1997) Biophys Chem 64:127
25. Schuck P, Minton AP (1996) Anal Biochem 240:262
26. Schuck P (1996) Biophys J 70:1230
27. Sjolander S, Urbaniczky C (1991) Anal Chem 63:2338
28. Edwards DA (2001) Bull Math Biol 63:301